KNOTS IN STELLAR JETS : CROSSING
SHOCKS OR INTERNAL WORKING SURFACES ?

A.C. Raga[1]

Canadian Institute for Theoretical Astrophysics

and

A. Noriega-Crespo

Astronomy Department, University of Washington

Received 1991 April 3

RESUMEN

En este artículo describimos las implicaciones observacionales de modelos teóricos de la formación de nudos en jets estelares. En particular, presentamos predicciones de los desplazamientos espaciales entre la emisión en Hα y [S II] obtenidas con dos modelos : un modelo de "choques internos" (en el cual los nudos corresponden a pares de choques incidentes y reflejados) y un modelo de "superficies de trabajo internas" (en el cual los nudos corresponden a pares de choques formados como consecuencia de una variabilidad temporal de la fuente del jet). Una comparación entre las predicciones teóricas y las observaciones del objeto Herbig-Haro HH 34 parece favorecer al segundo modelo.

ABSTRACT

We discuss the observational implications of theoretical models for the formation of knots in stellar jets. In particular, we present predictions of the spatial offsets between the Hα and the [S II] emission from two possible models : a "crossing shock" model (in which the knots correspond to incident/reflected shock pairs), and an "internal working surface" model (in which the knots correspond to shock pairs that result from a time-variability of the outflow source). A comparison of the theoretical predictions with observations of the jet-like Herbig-Haro object HH 34 appears to favour the second of these scenarios.

Key words: **HERBIG-HARO OBJECTS – SHOCK WAVES**

I. INTRODUCTION

The subclass of Herbig-Haro (H-H) objects known as "stellar jets" have a structure of a-ligned, more or less evenly spaced knots (see, e. g., Reipurth *et al.* 1986; Mundt, Brugel, and Bührke 1987; Reipurth 1989). A large part of the theoretical effort on stellar jets has been focussed on the interpretation of this condensation structure.

It was first proposed by Königl (1982) that the excitation produced by incident/reflected shock pairs in a jet flow might be responsible for the emission spectrum of H-H objects. Models of steady jets show that initially over or underexpanded jets have a series of incident/reflected crossing shock pairs, which do result in the production of

aligned condensations in the predicted emission line intensity maps (Falle, Innes, and Wilson 1987; Raga *et al.* 1991). Incident/reflected shock pairs could also be formed as a result of instabilities in the jet/environment boundary (see, e. g., the discussion of Bührke, Mundt, and Ray 1988; and Blondin, Fryxell and Königl 1990).

An alternative possibility is that the knots in stellar jets might correspond to "internal working surfaces". In this scenario, perturbations in the ejection velocity result in the formation of two-shock structures (reminiscent of the working surface at the head of the jet) that travel downstream along the jet flow. Rees (1978) proposed this scenario for extragalactic jets, and Raga *et al.* (1990) have studied it in the context of stellar jets.

In this paper, we present predictions of the Hα and [S II] 6717+31 emission for both of the scenar-

1. Present address: The University, Manchester, U.K.

ios described above. The crossing shocks are modeled with the steady, axisymmetric, nonadiabatic hydrodynamical code of Raga, Binette, and Cantó (1990). We model the internal working surfaces under the assumption that the leading shock (the bowshock) dominates the emission, so that the simple formulation of Raga and Böhm (1985) can be used.

In particular, we discuss the offsets obtained between the Hα and [S II] intensity maxima. This prediction is useful for comparisons with observations, because even though the knots are at best only marginally resolved in images of stellar jets, very small offsets ($\sim$ 0.5") can be quite accurately measured. We then compare these predictions with the results obtained for HH 34.

II. CROSSING SHOCKS IN STEADY JETS

Raga *et al.* (1990) have developed a steady, nonadiabatic jet model in which the nonequilibrium ionization and cooling are considered. From these models it is possible to obtain predictions of the intensity emitted along the jet (integrated over the jet's cross section) in any emission line.

In Figure 1, we show the Hα and the [S II] 6717+6731 intensities as a function of distance from the source. The results correspond to a jet with initial velocity $v_j^0 = 150$ km s^{-1}, hydrogen number density $n_H^0 = 10^4$ cm^{-3}, temperature $T_j^0 = 9000$ K, radius $r_j^0 = 10^{16}$ cm, and jet to environment pressure ratio $P_j^0/P_e = 20$ (the environment is assumed to be homogeneous). We assume that at $X = 0$ the jet has a "top hat" cross section and is parallel to the axis, and that the gas is in coronal ionization equilibrium (i.e., collisional ionizations balanced by radiative and dielectronic recombinations) at the initial temperature T_j^0. These assumptions are completely equivalent to the ones of Raga *et al.* (1990).

The intensity maxima resulting from the incident/reflected crossing shock cells are clearly seen in Figure 1 (see also Raga *et al.* 1991). From this figure, it is also clear that the positions of the Hα intensity peaks do not coincide with the [S II] peaks.

Let us define the Hα/[S II] offsets (normalized to the size of the knots) as :

$$\Delta_1 = \frac{X_{H1} - X_{S1}}{W_{S1}}, \qquad (1)$$

$$\Delta_2 = \frac{X_{H2} - X_{S2}}{W_{S2}}, \qquad (2)$$

where X_{H1} and X_{S1} are the positions of the Hα and [S II] peaks of the first crossing shock cell, and X_{H2} and X_{S2} are the corresponding parameters for
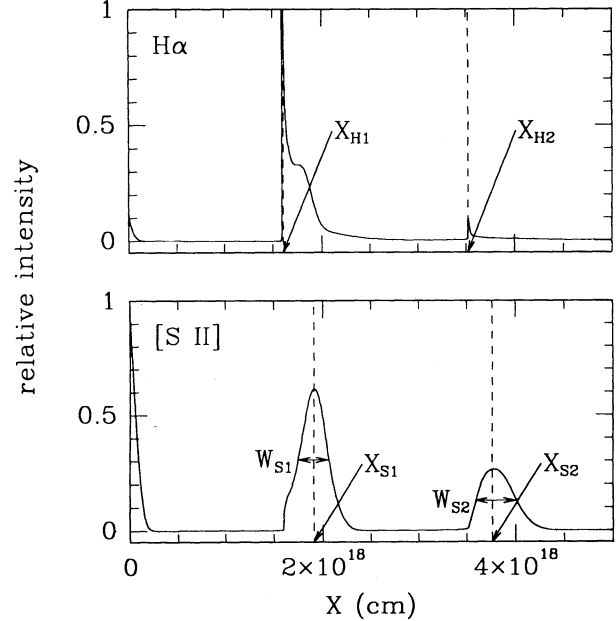

Fig. 1. Hα (top) and [S II] 6717+6731 (bottom) intensities along a jet flow (integrated over the cross section of the jet). The intensities are given in arbitrary units. The results shown have been obtained from a v_j^0 = 150 km s^{-1}, P_j^0/P_e = 20 steady jet model (the other parameters of the flow are discussed in the text). X corresponds to the distance measured from the source, along the flow axis. The positions X_{H1} and X_{H2} of the Hα intensity maxima, and the positions X_{S1} and X_{S2} of the [S II] intensity maxima of the first and second crossing shock cells (respectively) are indicated in the diagrams. The values of the full width half maximum W_{S1} and W_{S2} of the [S II] peaks of the first and second crossing shock cells (respectively) are indicated in the bottom diagram.

the second crossing shock cell. W_{S1} and W_{S2} are the FWHM of the [S II] emission (measured along the jet axis) of the first and second crossing shock cells (respectively). These parameters are clearly indicated in Figure 1.

In Figure 2, we show the values of Δ_1 and Δ_2 for four different jet models. These models have parameters identical to the ones of the model discussed above, except that different initial jet to environment pressure ratios (P_j^0/P_e = 2.5, 10, 20 and 30) are considered.

We see that for low initial jet to environment pressure ratios, the offsets between the Hα and [S II] peaks are small relative to the size of the knots (i.e., for P_j^0/P_e = 2.5, we have $\Delta_1 \approx \Delta_2 \approx -0.1$). For $P_j^0/P_e \geq 10$, we have $\Delta_1 \sim -0.9$ and $\Delta_2 \sim -0.6$. In other words, for all models we see that the Hα intensity peaks are closer to the source than the [S II] intensity peaks. As we will see in §IV, this
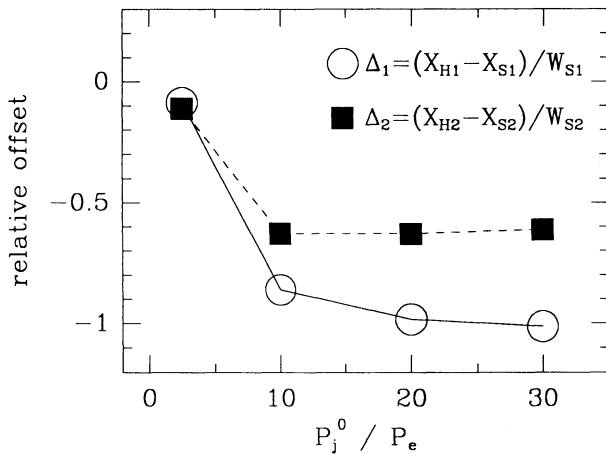
Fig. 2. Normalized Hα/[S II] offsets Δ_1 and Δ_2 (corresponding to the first and second crossing shock cells, respectively) for steady jet models with $v_j^0 = 150$ km s^{-1} and initial jet to environment pressure ratios $P_j^0/P_e = 2.5, 10, 20$ and 30. It is clear that for all models, only negative Δ values are obtained.

result is in disagreement with the observations of the HH 34 jet.

III. INTERNAL WORKING SURFACES

Raga et al. (1990) show that time changes in the injection velocity can result in the formation of internal working surfaces in the jet flow. As is clearly seen in the adiabatic flow simulations of Wilson (1984), these working surfaces consist of two shocks: a Mach disk, and a bowshock (which is driven into the downstream region of the jet and into the environment).

In order to calculate the emission from such structures, it would in principle be necessary to carry out a full time-dependent simulation of the nonadiabatic flow (such as the ones of Raga 1988; Blondin, Königl, and Fryxell 1989). However, in the present paper we limit ourselves to a much simpler calculation.

We assume that the emission of the internal working surface is dominated by the contribution from the bowshock. As discussed, e.g., by Hartigan (1989) and Raga (1988), this is indeed the case provided that the density upstream of the working surface (i.e., closer to the source) is considerably higher than the downstream density. Of course, it is at this time unclear whether or not this might be the actual case in stellar jets.

We further assume that the bowshock is moving into a uniform density medium, and that its shape is described by the simple, parametrized form derived by Raga and Böhm (1985). Under these as-

sumptions, we can use the simple, quasi-one dimensional formulation (which consists of approximating the emission from the bowshock as a superposition of locally one-dimensional recombination regions) of Hartmann and Raymond (1984).

In this way, we can carry out predictions of emission line intensities (integrated over the cross section of the bowshock) as a function of position along the symmetry axis (similar predictions have been discussed by Noriega-Crespo, Böhm, and Raga 1989, 1990). In Figure 3, we show the prediction of the Hα and [S II] intensities as a function of distance X from the head of the bowshock (given in units of the stagnation radius R_b of the bowshock). We have assumed a preshock atom and ion number density $n = 100$ cm^{-3}, and a velocity $V = 100$ km s^{-1} for the bowshock. For calculating the emission we have used the intensities from one-dimensional shocks predicted by Hartigan, Raymond, and Hartmann (1987).

If we believe that the emission from an internal working surface in a jet resembles the predictions from our simple bowshock models, the results shown in Figure 3 would correspond to the emission line intensities measured along the jet, going through a knot. The direction away from the jet source is towards positive X. We can then use these results to calculate the offsets between the positions of the Hα and [S II] intensity maxima (normalized to the FWHM of the [S II] emission), in an analogous way to what we have done in §II (see equations 1 and 2).

In Figure 4, we show the normalized Hα/[S II] offsets Δ_P and Δ_E for bowshock models of velocities $V = 30, 50, 80$ and 100 km s^{-1}. The values of Δ_P have been calculated assuming that the pre-bowshock gas has fully ionized hydrogen, and the values of Δ_E represent bowshocks with "equilibrium preionization" (i.e., the preshock ionization is determined by the photoionization due to the postshock emission, see Hartigan et al. 1987). Due to the fact that stellar jets are observed to be mostly neutral, the Δ_E values might be more representative of the actual conditions we are interested in.

The Δ_E values shown in Figure 4 indicate that for low bowshock velocities ($V < 80$ km s^{-1}) the Hα emission peaks farther away from the source than the [S II] emission (for a definition of the normalized offsets Δ see equations 1 and 2). However, the converse is true for larger shock velocities ($V > 80$ km s^{-1}, see Figure 4).

As we have mentioned above, internal working surfaces in jets will actually have emission not only from the bowshock, but also from a Mach disk. We find that even if we constrain ourselves to the subset of "bowshock dominated" working surfaces
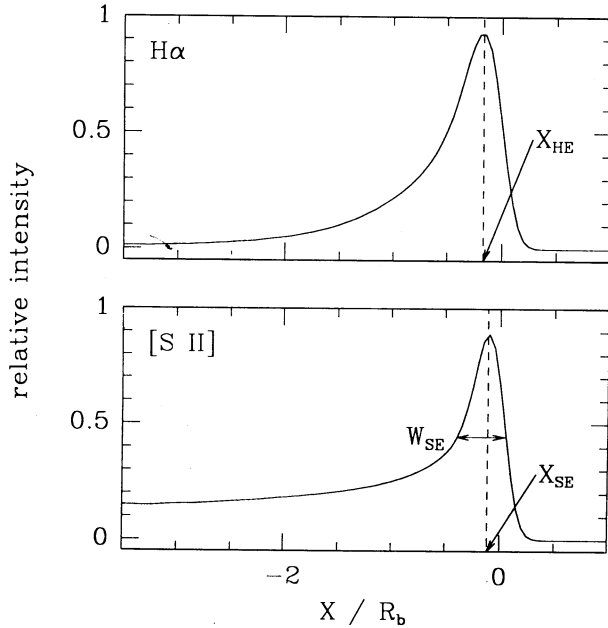
Fig. 3. Hα (top) and [S II] 6717+6731 (bottom) intensities as a function of position along the bowshock axis (integrated over the cross section of the bowshock, see the text). The intensities are given in arbitrary units. X is the position along the symmetry axis, and $X = 0$ corresponds to the position of the head of the bowshock (the distances are given in units of the stagnation region radius of the bowshock R_b). The direction to the source is towards negative X values. The results shown have been obtained from a $V = 100$ km s^{-1} bowshock model with "equilibrium preionization" (see the text). The positions X_{HE} and X_{SE} of the Hα and [S II] intensity maxima (respectively) are shown in the diagrams. Also shown in the bottom diagram is W_{SE} the full width half maximum of the [S II] intensity.

Fig. 4. Normalized Hα/[S II] offsets Δ_P and Δ_E (corresponding to bowshock models with fully preionized hydrogen, and with "equilibrium preionization", respectively) for bowshock models with velocities $V = 30$, 50, 80 and 100 km s^{-1}. Both positive and negative Δ values are obtained for different models.

(which are obtained only for appropriate upstream to downstream density ratios, see above) we can obtain both positive and negative values of Δ.

This possibility of having both positive and negative Δ values is an important difference between internal working surface models and crossing shock models (for which we only obtain negative Δ values, see §II). In the following section, we discuss how this result can be used to provide an interesting observational constraint on the mechanism for the formation of knots in stellar jets.

IV. DISCUSSION: A COMPARISON WITH OBSERVATIONS OF HH 34

We have presented a discussion of the properties of the Hα and [S II] emission predicted from two different models for the formation of knots in stellar jets. We have shown that steady crossing shock models predict that the Hα emission of the knots
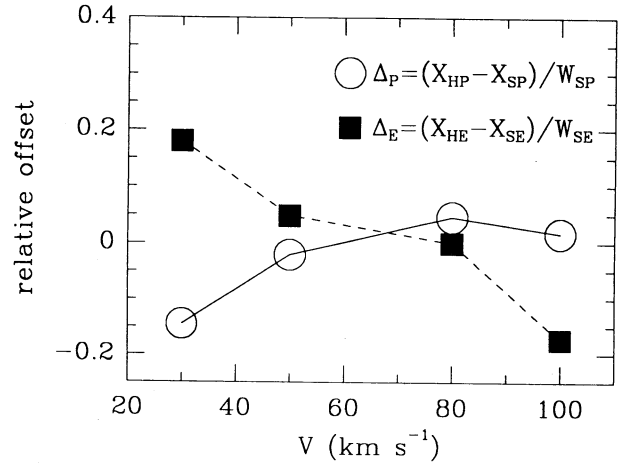
peaks closer to the source than the [S II] emission. On the other hand, we find that for models in which the knots are identified with "internal working surfaces" in the flow, both positive and negative Hα/[S II] offsets are in principle possible.

We have measured the normalized Hα/[S II] offsets, Δ, for the knots in the jet of HH 34, in order to compare it with our theoretical predictions. The offsets are defined by $\Delta = (X_{H\alpha} = X_{[SII]})/W_{[SII]}$ (where $X_{H\alpha}$ and $X_{[SII]}$ are the distances from the source to the knots, and $W_{[SII]}$ is the [S II] FWHM measured along the jet axis for the corresponding knot). The positions and the FWHM of the knots were measured from CCD images takes by one of us at the KPNO 2.1-m telescope (see Raga and Mateo 1988, for details of the observations).

We reproduce these Δ values in Figure 5, where we show the normalized Hα/[S II] offsets as a function of distance from the source for the brighter knots of the HH 34 jet. The uncertainty in positions of the knots is ~ 0.3 pixel and the uncertainty for the FWHM is approximately 1/10 of its values. The error bars in Figure 5 are based on both uncertainties. We have not included the knots associated with the leading working surface of HH 34 due to the complexity of the flow. The brightest features in the working surface, however, show a clear shift between the Hα and [S II] CCD images, as well as with respect to the [O III] 5007 image (see e.g., Fig. 9, Bürke, Mundt, and Ray 1988). The knots in the HH 34 jet show Hα/[S II] offsets with values $\Delta \sim 0.2 - 0.5$, with the exception of the knot farthest away from the source which shows a negative Δ value.
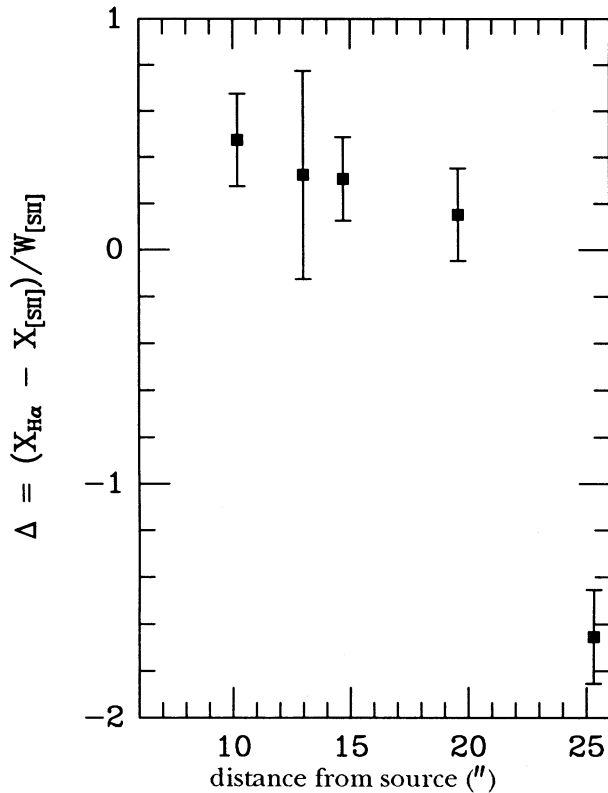
Fig. 5. Normalized Hα/[S II] offsets for the knots along the HH 34 jet (see the text for details).

our models for the internal working surfaces are extremely simplified, and more detailed calculations will have to be carried out in order to better understand the characteristics of the emission from such structures.

From this result, we would conclude that the observed positive values of the Hα/[S II] offset cannot be explained by a "crossing shock model" for the knots of the jet. On the other hand, the observations might be consistent with an "internal working surface model" for the knots (for which both positive and negative Δ values are possible, see above).

This conclusion, however is based on models with important simplifications. For example, our crossing shock models are based on the assumption of a steady state flow. Time-dependent effects (see, e.g., Blondin *et al.* 1990) might produce important differences in the predicted line intensities. Also,

REFERENCES

Blondin, J.M., Fryxell, B.A., & Königl, A. 1990, ApJ, 360, 370
Blondin, J.M., Königl, A., & Fryxell, B.A. 1989, ApJ, 337, L37
Bührke, T., Mundt, R., & Ray, T.P. 1988, A&A 200, 99
Falle, S.A.E.G., Innes, D., & Wilson, M.J. 1987, MNRAS, 225, 741
Hartigan, P. 1989, ApJ, 399, 987
Hartigan, P., Raymond, J., & Hartmann, L. 1987, ApJ, 316, 323
Hartmann, L., & Raymond, J.C. 1984, ApJ, 276, 560
Königl, A. 1982, ApJ, 261, 115
Mundt, R., Brugel, E.W., & Bührke, T. 1987, ApJ, 319, 275
Noriega-Crespo, A., Böhm, K.H., & Raga, A.C. 1989, AJ, 98, 1388
_____. 1990, AJ, 99, 1918
Raga, A.C. 1988, ApJ, 335, 820
Raga, A.C., & Böhm, K.H. 1985, ApJS, 58, 201
Raga, A.C.,& Mateo, M. 1988, AJ, 95, 543
Raga, A.C., Binette, L., & Cantó, J. 1990, ApJ, 360, 612
Raga, A.C., Biro, S., Cantó, J., & Binette, L. 1991, RevMexAA, 22, 243
Raga, A.C., Cantó, J., Binette, L., & Calvet, N. 1990, ApJ, 364, 601
Rees, M.J. 1978, MNRAS, 184, 61
Reipurth, B. 1989, in ESO Workshop on Low Mass Star Formation and Pre-Main Sequence Objects, ed. B. Reipurth, p. 247
Reipurth, B., Bally, J., Graham, J.A., Lane, A., & Zealy, W.J. 1986, A&A, 164, 51
Wilson, M.J. 1984, MNRAS, 209, 923

Alberto Noriega-Crespo: Astronomy Department, FM-20, University of Washington, Seattle, WA 98195, USA.
Alejandro C. Raga: Astronomy Department, The University, Manchester M13 9PL, U.K.